6 Appendix A: Dispersion Relations

Bernhard Schmidt, Peter Schmüser et al., preliminary version

A dispersion relation is an integral formula relating a dispersive process to an absorptive process. An example is the relation between the refractive index $n(\omega)$ of an optical medium and its extinction coefficient $k(\omega)$, or the relation between real part and imaginary part of the dielectric function of a solid. Dispersion relations follow rigorously from causality. In this appendix we follow closely the book *Optical Properties of Solids* by F. Wooten [18] but we go into more detail and present several mathematical proofs that are missing in [18]. A comprehensive treatment can be found in [27].

6.1 Basics of complex analysis

Cauchy-Riemann equations
The set of complex numbers $z = x + iy$ is called $\mathbf{C}$. These numbers can be depicted as points in a plane (x, iy). A function $f(z)$ is called analytic (or holomorphic) in an open subset U of $\mathbf{C}$ if the differential quotient exists

$$\frac{df}{dz} = \lim_{\Delta z \to 0} \frac{f(z + \Delta z) - f(z)}{\Delta z} \,. \tag{39}$$

The differential quotient is defined in the same way as in real analysis, but the limit can be approached from many different directions. This has far-reaching consequences. Separating the complex function into its real and imaginary parts

$$f(z) = f(x + iy) = u(x, y) + iv(x, y) \tag{40}$$

one can prove that $f(z)$ is analytic if and only if the **Cauchy-Riemann differential equations** are fulfilled

$$\frac{\partial u}{\partial x} = \frac{\partial v}{\partial y} \,, \qquad \frac{\partial u}{\partial y} = -\frac{\partial v}{\partial x} \,. \tag{41}$$

Analytic functions have many remarkable properties that are not valid for real functions. For example the derivative of an analytic function is again analytic which means that analytic functions are infinitely often differentiable.

Cauchy Integral Theorem and Residue Theorem
The Cauchy integral theorem is an important statement about line integrals in the complex plane $\mathbf{C}$. If two different paths connect the same start and end points, and if the function is analytic in an open set containing the two paths, then these two path integrals of the function yield the same value. The theorem is usually formulated for closed paths:
Let U be an open subset of $\mathbf{C}$ which is simply connected, let $f : U \to \mathbf{C}$ be an analytic function, and let Γ be a closed loop. Then the line integral over the closed loop vanishes

$$\oint_\Gamma f(z)dz = 0 \qquad\qquad \textit{Cauchy Integral Theorem} \,. \tag{42}$$

Consider now the function $g(z) = f(z)/(z - z_0)$ where z_0 is an arbitrary point inside the closed loop Γ. The function $g(z)$ is analytic except for a small vicinity around the pole at z_0. The Residue Theorem states

$$\oint_\Gamma \frac{f(z)}{z - z_0} dz = 2\pi\, i f(z_0) \equiv 2\pi\, i \,\mathrm{Res}(f, z_0) \quad \textit{Residue Theorem} \,. \tag{43}$$

This is easy to verify for a small circle centered at z_0 whose radius a tends to zero. On the circle we have

$$\begin{aligned} z &= z_0 + ae^{i\theta}, \quad dz = i\,ae^{i\theta}d\theta \\ \lim_{a\to 0}\oint_{\text{circ}} \frac{f(z)}{z-z_0}dz &= f(z_0)\lim_{a\to 0}\int_0^{2\pi}\frac{1}{ae^{i\theta}}\,i\,ae^{i\theta}d\theta = 2\pi\,i f(z_0)\,. \end{aligned}$$

Computation of an important integral
In the next section 6.2 an integral of the type

$$\int_{-\infty}^{\infty}\frac{e^{ix}}{x-x_0}dx$$

appears. The integrand has a singularity at $x = x_0$. We want to show how such integrals along the real axis can be evaluated by going into the complex plane and using the Cauchy and Residue Theorems. For this purpose we consider a closed integration path Γ consisting of three parts (see Fig. 30):
(1) A large semicircle Γ_1 of radius R which is centered at the origin $z = 0$,
(2) a straight line Γ_2 along the real axis from $x = -R$ to $x = x_0 - \varepsilon$ and from $x = x_0 + \varepsilon$ to $x = +R$,
(3) a small semicircle Γ_3 of radius ε which is centered at x_0.

Step 1 Consider a function $f(z)$ which is analytic in the upper half plane $y \geq 0$, except for a finite number of poles, and which vanishes asymptotically

$$\lim_{|z|\to\infty} f(z) = 0 \quad \text{for} \quad y \geq 0\,. \tag{44}$$

Statement: The line integral of the function $f(z)e^{iz}$ along the semicircle Γ_1 tends to zero in the limit $R \to \infty$:

$$\lim_{R\to\infty}\int_{\Gamma_1} f(z)e^{iz}dz = 0\,. \tag{45}$$

This statement is by no means obvious. Because of (44), the integrand tends to zero with increasing radius of the semicircle, $|f(z)e^{iz}| \to 0$ for $|z| \to \infty$ and $y > 0$, but at the same time the path length of the semicircle tends to infinity.

Proof: The proof of (45) goes as follows (see H. Cartan [29]). On the semicircle we have

$$z = Re^{i\theta}\,, \quad dz = iRe^{i\theta}d\theta\,, \quad |e^{iz}| = e^{-R\sin\theta}\,.$$

An upper limit for the integral is

$$\left|\int_{\Gamma_3} f(z)e^{iz}dz\right| \leq \int_0^{\pi}|f(Re^{i\theta})|e^{-R\sin\theta}Rd\theta \leq M(R)\int_0^{\pi}e^{-R\sin\theta}Rd\theta = 2M(R)\int_0^{\pi/2}e^{-R\sin\theta}Rd\theta$$

with

$$M(R) = \max_{0\leq\theta\leq\pi}(|f(Re^{i\theta})|)\,.$$

In the interval $0 \leq \theta \leq \pi/2$ one has $\sin\theta \geq 2\theta/\pi$, hence

$$\int_0^{\pi/2}e^{-R\sin\theta}Rd\theta \leq \int_0^{\pi/2}e^{-2\theta R/\pi}Rd\theta = \pi/2\,.$$

The result is

$$\left|\int_{\Gamma_1} f(z)e^{iz}dz\right| \leq \pi\,M(R) \qquad \text{and} \quad \lim_{R\to\infty}M(R) = 0\,.$$

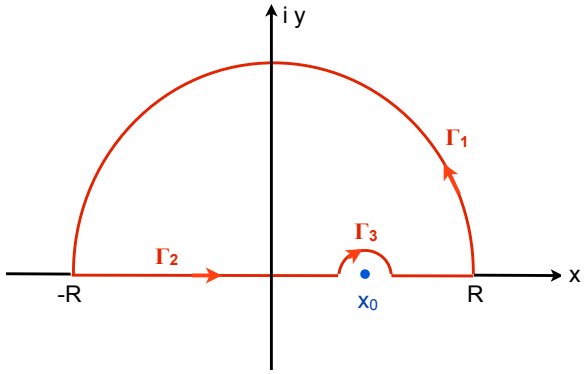

Figure 30: The closed integration path Γ.

Therefore

$$\lim_{R\to\infty}\int_{\Gamma_1} f(z)e^{iz}dz = 0 \qquad \text{qed}\,.$$

Specifically, the function $f(z) = 1/(z - x_0)$ fulfills the condition (44). Hence

$$\lim_{R\to\infty}\int_{\Gamma_1}\frac{e^{iz}}{z-x_0}dz = 0\,. \tag{46}$$

Step 2 Next we want to evaluate the closed-loop integral

$$\oint_{\Gamma}\frac{e^{iz}}{z-x_0}dz\,.$$

The function $1/(z - x_0)$ has a pole at $z = x_0$ but is analytic elsewhere. Next we show that e^{iz} is analytic in the entire complex plane. We prove this for the more general case $e^{iz\tau}$ where τ is a real number. For this purpose we write

$$e^{iz\tau} = e^{i(x+i\,y)\tau} = u(x,y) + i\,v(x,y)\,.$$

The real functions $u(x, y)$ and $v(x, y)$ are

$$u(x,y) = \cos(x\tau)\,e^{-y\tau}, \qquad v(x,y) = \sin(x\tau)\,e^{-y\tau}\,.$$

It is easy to verify that that they fulfill the Cauchy-Riemann differential equations

$$\frac{\partial u}{\partial x} = -\tau\,\sin(x\tau)\,e^{-y\tau} = \frac{\partial v}{\partial y}\,, \qquad \frac{\partial u}{\partial y} = -\tau\,\cos(x\tau)\,e^{-y\tau} = -\frac{\partial v}{\partial x}\,.$$

This proves that $f(z) = e^{iz\tau} = e^{i(x+i\,y)\tau} = u(x, y) + i\,v(x, y)$ is an analytic function of the complex variable $z = x + i\,y$

The pole at x_0 is avoided by choosing the closed integration path Γ shown in Fig. 30. There is no singularity inside the loop, hence from Cauchy's formula (42)

$$\oint_{\Gamma}\frac{e^{iz}}{z-x_0}dz = \int_{\Gamma_1}\frac{e^{iz}}{z-x_0}dz + \int_{\Gamma_2}\frac{e^{iz}}{z-x_0}dz + \int_{\Gamma_3}\frac{e^{iz}}{z-x_0}dz = 0\,.$$

The three path integrals are evaluated in the limit $\varepsilon \to 0$ and $R \to \infty$.

Because of (46) we get

$$\int_{\Gamma_2} \frac{e^{iz}}{z-x_0} dz = -\int_{\Gamma_3} \frac{e^{iz}}{z-x_0} dz\,.$$

The integral over the small semicircle is readily evaluated

$$\begin{aligned} z &= x_0 + \varepsilon\, e^{i\theta}, \quad dz = i\,\varepsilon\, e^{i\theta} d\theta \\ \lim_{\varepsilon\to 0} \int_{\Gamma_3} \frac{e^{iz}}{z-x_0} dz &= e^{ix_0} \lim_{\varepsilon\to 0} \int_{2\pi}^{\pi} \frac{1}{\varepsilon\, e^{i\theta}}\, i\,\varepsilon e^{i\theta} d\theta = -\pi\, i e^{ix_0}\,. \end{aligned}$$

The integral over the path Γ_2 is therefore in the limit $R \to \infty$ and $\varepsilon \to 0$

$$\int_{\Gamma_2} \frac{e^{iz}}{z-x_0} dz = \lim_{\varepsilon\to 0} \left[\int_{-\infty}^{x_0-\varepsilon} \frac{e^{iz}}{z-x_0} dz + \int_{x_0+\varepsilon}^{\infty} \frac{e^{iz}}{z-x_0} dz \right] = i\,\pi\, e^{ix_0}\,.$$

The path Γ_2 is along the real axis, hence $z = x$ on Γ_2. It is customary to define the principal value of an integral, denoted by the letter $\mathcal{P}$, by approaching the singularity at x_0 symmetrically from both sides:

$$\mathcal{P} \int_{-\infty}^{\infty} \frac{e^{ix}}{x-x_0} dx = \lim_{\varepsilon\to 0} \left[\int_{-\infty}^{x_0-\varepsilon} \frac{e^{ix}}{x-x_0} dx + \int_{x_0+\varepsilon}^{\infty} \frac{e^{ix}}{x-x_0} dx \right] \tag{47}$$

The important result is

$$\boxed{\mathcal{P} \int_{-\infty}^{\infty} \frac{e^{ix}}{x-x_0} dx = i\,\pi\, e^{ix_0}\,.} \tag{48}$$

6.2 Linear Response Functions

We restrict ourselves to *linear* systems: The response X of the system under consideration depends linearly on the stimulus S. The response can be calculated by a convolution integral

$$X(t) = \int_{-\infty}^{+\infty} G(t-t')S(t')dt'\,. \tag{49}$$

$G(t-t')$ is called the response function. Nonlinear systems, for example nonlinear crystals for frequency doubling of laser light, are not treated here.

An example of a linear system is a dielectric medium in which the induced polarization (the response) depends linearly on the applied electric field (the stimulus):

$$\boldsymbol{P} = \chi_e \varepsilon_0 \boldsymbol{E}\,.$$

The electric susceptibility χ_e is the response function in this case.

Causality puts an important constraint on G. There cannot be any response before there is a stimulus, hence we must request

$$G(t-t') = 0 \qquad \text{for} \quad t < t'\,. \tag{50}$$

The Fourier transforms are

$$\tilde{X}(\omega) = \int X(t) e^{i\omega t} dt\,, \quad \tilde{G}(\omega) = \int G(\tau) e^{i\omega\tau} d\tau\,, \quad \tilde{S}(\omega) = \int S(t) e^{i\omega t} dt \tag{51}$$

with $\tau = t - t'$. Using Eq. (49) we find

$$\begin{aligned} \tilde{X}(\omega) &= \int dt\, X(t) e^{i\omega t} = \int dt \int dt' \left[e^{i\omega t}\, G(t-t') S(t') \right] \\ &= \int dt' \underbrace{\left(\int dt\, G(t-t') e^{i\omega(t-t')} \right)}_{\tilde{G}(\omega)} S(t') e^{i\omega t'} = \tilde{G}(\omega)\, \tilde{S}(\omega)\,. \end{aligned}$$

The important result is: the Fourier transform of the system response (given by the convolution integral (49)) is equal to the product of the Fourier transforms of the response function and the stimulus

$$\tilde{X}(\omega) = \tilde{G}(\omega)\,\tilde{S}(\omega)\,. \tag{52}$$

Complex ω plane
Now we define complex frequencies. Let $\omega = \omega_\mathrm{r} + i\,\omega_\mathrm{i}$ be a complex number. The Fourier integral (51) defines $\tilde{G}(\omega)$ as a function of the real variable ω. We generalize this definition to comprise complex frequencies as well:

$$\tilde{G}(\omega_\mathrm{r} + i\,\omega_\mathrm{i}) = \int G(\tau) e^{i\omega_\mathrm{r}\tau} e^{-\omega_\mathrm{i}\tau} d\tau\,. \tag{53}$$

We know from the previous discussion that $e^{i\omega\tau}$ is an analytic function of the complex variable $\omega = \omega_\mathrm{r} + i\,\omega_\mathrm{i}$, and hence the response function $\tilde{G}(\omega)$ is analytic. So we are allowed to apply Eq. (48):

$$\mathcal{P}\int_{-\infty}^{\infty} \frac{\tilde{G}(\omega)}{\omega - \omega_0} d\omega = i\pi\tilde{G}(\omega_0)\,. \tag{54}$$

Separating real and imaginary part we obtain the important Kramers-Kronig dispersion relations

$$\Re(\tilde{G}(\omega_0)) = \frac{1}{\pi}\,\mathcal{P}\int_{-\infty}^{\infty} \frac{\Im(\tilde{G}(\omega))}{\omega - \omega_0} d\omega\,, \quad \Im(\tilde{G}(\omega_0)) = -\frac{1}{\pi}\,\mathcal{P}\int_{-\infty}^{\infty} \frac{\Re(\tilde{G}(\omega))}{\omega - \omega_0} d\omega\,. \tag{55}$$

This shows that real part and imaginary part of the response function are intimitely connected. The real part can be computed by a principal value integral over the imaginary part, and the imaginary part can be computed by a principal value integral over the real part.
An important application is the relation between real part and imaginary part of the electric susceptibility $\chi_e(\omega) = \varepsilon(\omega) - 1 = \varepsilon_1(\omega) - 1 + i\,\varepsilon_2(\omega)$ of a solid (see [18])

$$\varepsilon_1(\omega) - 1 = \frac{1}{\pi}\,\mathcal{P}\int_{-\infty}^{\infty} \frac{\varepsilon_2(\omega')}{\omega' - \omega} d\omega'\,, \quad \varepsilon_2(\omega) = -\frac{1}{\pi}\,\mathcal{P}\int_{-\infty}^{\infty} \frac{\varepsilon_1(\omega') - 1}{\omega' - \omega} d\omega'\,. \tag{56}$$

Here we have replaced ω_0 by ω and renamed the integration variable from ω to ω'.

6.3 Dispersion relation for absolute magnitude and phase

The dispersion relation (55) requires the knowledge of either the real part or the imaginary part of the response function. However, in many cases only the absolute magnitude is known, so it is desirable to derive a relation allowing to compute the phase. Following [18] we consider the reflection of an electromagnetic wave from a solid at normal incidence.

The complex reflectivity amplitude $r(\omega)$ relates the Fourier components of incident and reflected electric field

$$\tilde{E}_r(\omega) = r(\omega)\tilde{E}_i(\omega)\,. \tag{57}$$

In terms of the response function the reflectivity amplitude can be expressed as

$$r(\omega) = \rho(\omega)e^{i\Phi(\omega)} = \int_{-\infty}^{\infty} G(\tau)e^{i\omega\tau}d\tau = \int_{0}^{\infty} G(\tau)e^{i\omega\tau}d\tau\,. \tag{58}$$

We know already that $e^{i\omega\tau}$ and thus $r(\omega)$ are analytic functions in the entire $\omega = \omega_\mathrm{r} + i\omega_\mathrm{i}$ plane. Moreover they are bounded in the upper half plane ($\omega_\mathrm{i} > 0$) since $e^{-\omega_\mathrm{i}\tau} \to 0$ for $\omega_\mathrm{i} \to \infty$.

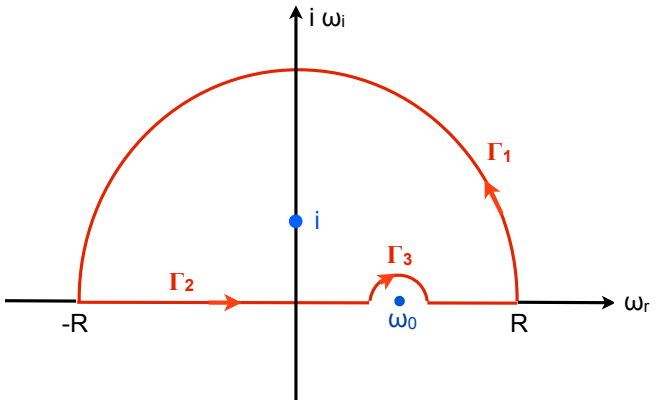

Figure 31: The closed integration path Γ for the auxiliary function (59).

Unfortunately one cannot use the Kramers-Kronig relation because in spectroscopic experiments one usually measures only the absolute square of the reflectivity amplitude $R(\omega) = |r(\omega)|^2 = (\rho(\omega))^2$ but not its phase nor its real or imaginary part. To determine the phase $\Phi(\omega)$ it is convenient to derive a dispersion relation for

$$\ln(r(\omega)) = \ln(\rho(\omega)) + i\Phi(\omega)\,.$$

We want to apply the Residue Theorem for the closed loop shown in Fig. 31. This needs a lot of work, and some problems arise.

(1) $\ln(r(\omega))$ is not allowed to have a singularity in the upper half plane so we must require $r(\omega) \neq 0$ for any ω with a positive imaginary part. Wooten [18] argues that $r(\omega)$ must be nonzero for physical reasons but we are not convinced that his argument applies also for "unphysical" complex frequencies. In case of bunch form factors, complex zeros in the upper half plane may indeed exist, and they have a strong impact on the phase determination, see Sect. 6.4.2 and Appendix B.

(2) A severe problem is that the reflectivity becomes zero at infinite frequency, hence $|\ln(\omega)|$ diverges for $|\omega| \to \infty$. This means that the line integral of $\ln(r(\omega))$ over the semicircle Γ_1 diverges as well. To circumvent this difficulty one defines the auxiliary function

$$f_{\rm aux}(\omega) = \frac{(1+\omega_0\omega)\ln(r(\omega))}{(1+\omega^2)(\omega_0-\omega)} = \frac{1}{\omega-i}\,\frac{(1+\omega_0\omega)\ln(r(\omega))}{(\omega+i)(\omega_0-\omega)} \tag{59}$$

with a real positive frequency ω_0. Furthermore one makes the assumption that asymptotically $|r(\omega)|$ obeys an inverse power law:

$$|r(\omega)| = b|\omega|^{-m} \quad \text{with} \quad m > 0 \quad (|\omega| \to \infty). \tag{60}$$

Then the function $f_{\rm aux}$ behaves asymptotically as

$$|f_{\rm aux}(\omega)| = \left|\frac{(1+\omega_0\omega)(-m\ln(\omega)+\ln(b))}{(1+\omega^2)(\omega_0-\omega)}\right|\,.$$

On the large semicircle Γ_1 we have

$$\omega = Re^{i\theta}\,, \quad |f_{\rm aux}(\omega)| \approx m\,\omega_0\left|\frac{\ln(R)}{R^2}\right|\,.$$

The pathlength of Γ_1 is πR, hence the integral of $f_{\rm aux}(\omega)$ over this semicircle vanishes if R tends to infinity:

$$\int_{\Gamma_1} f_{\rm aux}(\omega)d\omega \approx \pi\,m\,\omega_0\left|\frac{\ln(R)}{R}\right| \to 0\,. \tag{61}$$

Performing the integration of $f_{\rm aux}(\omega)$ along the closed loop shown in Fig. 31 we have to keep in mind that the auxiliary function has a pole at $\omega = i$ inside the loop. The Residue Theorem yields

$$\oint_\Gamma f_{\rm aux}(\omega)d\omega = 2\pi i \frac{1+i\omega_0}{2i(\omega_0 - i)} \ln(r(i)) = i\pi \ln(r(i))\,.$$

What is $r(i)$? From Eq. (58) follows that $r(i)$ is a real number which we call α:

$$r(i) = \int_{-\infty}^{\infty} G(\tau) e^{i^2\tau} d\tau = \int_{-\infty}^{\infty} G(\tau) e^{-\tau} d\tau \equiv \alpha\,.$$

Using the results of sect. 6.1 we find

$$\mathcal{P}\int_{-\infty}^{\infty} \frac{(1+\omega_0\omega)\ln(r(\omega))}{(1+\omega^2)(\omega_0-\omega)} d\omega + i\pi \ln(r(\omega_0)) = i\pi \ln(\alpha). \tag{62}$$

Inserting

$$r(\omega) = \rho(\omega) e^{i\Phi(\omega)}\,, \quad \ln(r(\omega)) = \ln(\rho(\omega)) + i\Phi(\omega) \tag{63}$$

we get

$$\mathcal{P}\int_{-\infty}^{\infty} \left[\frac{(1+\omega_0\omega)\ln(\rho(\omega)}{(1+\omega^2)(\omega_0-\omega)} + i\,\frac{(1+\omega_0\omega)\Phi(\omega)}{(1+\omega^2)(\omega_0-\omega)} \right] d\omega + i\pi \ln(\rho(\omega_0)) - \pi\Phi(\omega_0) = i\pi \ln(\alpha)\,.$$

The real part of this equation yields a first form of the desired dispersion relation

$$\Phi(\omega_0) = \frac{1}{\pi}\,\mathcal{P}\int_{-\infty}^{\infty} \frac{(1+\omega_0\omega)\ln(\rho(\omega))}{(1+\omega^2)(\omega_0-\omega)} d\omega\,. \tag{64}$$

Restriction to positive frequencies

The electric fields $E_i(t)$ and $E_r(t)$ are real while their Fourier transforms $\tilde{E}_i(\omega)$ and $\tilde{E}_r(\omega)$ are complex-valued functions. The Fourier transforms and their complex-conjugates $\tilde{E}_i^*(\omega)$ and $\tilde{E}_r^*(\omega)$ must satisfy the rule

$$\tilde{E}_i^*(\omega) = \tilde{E}_i(-\omega)\,, \quad \tilde{E}_r^*(\omega) = \tilde{E}_r(-\omega)$$

in order to obtain real functions $E_i(t)$ and $E_r(t)$. The complex reflectivity (63) obeys the same rule

$$r^*(\omega) = r(-\omega) \quad \Rightarrow \quad \rho(\omega) = \rho(-\omega)\,, \quad \Phi(-\omega) = -\Phi(\omega)\,. \tag{65}$$

The principal value integral is split up in two parts

$$\mathcal{P}\int_{-\infty}^{\infty} f_{\rm aux}(\omega)d\omega = \mathcal{P}\int_{-\infty}^{0} f_{\rm aux}(\omega)d\omega + \mathcal{P}\int_{0}^{\infty} f_{\rm aux}(\omega)d\omega\,.$$

In the integration over negative frequencies we make the replacement $u = -\omega$ and use $\rho(-u) = \rho(u)$

$$\mathcal{P}\int_{-\infty}^{0} \frac{(1+\omega_0\omega)\ln(\rho(\omega))}{(1+\omega^2)(\omega_0-\omega)} d\omega = \mathcal{P}\int_{0}^{\infty} \frac{(1-\omega_0 u)\ln(\rho(-u))}{(1+u^2)(\omega_0+u)} du = \mathcal{P}\int_{0}^{\infty} \frac{(1-\omega_0 u)\ln(\rho(u))}{(1+u^2)(\omega_0+u)} du\,.$$

Now we rename the integration variable u back into ω. Using

$$\frac{1+\omega_0\omega}{\omega_0-\omega} + \frac{1-\omega_0\omega}{\omega_0+\omega} = \frac{2\omega_0(1+\omega^2)}{\omega_0^2-\omega^2}$$

one can combine the two integrals and obtains

$$\Phi(\omega_0) = \frac{2\omega_0}{\pi}\,\mathcal{P}\int_0^\infty \frac{\ln(\rho(\omega))}{\omega_0^2-\omega^2}d\omega\,.$$

The integrand has a singularity at $\omega=\omega_0$. To cancel it one subtracts the expression

$$\frac{2\omega_0}{\pi}\,\mathcal{P}\int_0^\infty \frac{\ln(\rho(\omega_0))}{\omega_0^2-\omega^2}d\omega = \frac{2\omega_0\ln(\rho(\omega_0))}{\pi}\,\mathcal{P}\int_0^\infty \frac{1}{\omega_0^2-\omega^2}d\omega = 0\,.$$

It is easy to verify that this integral vanishes. With $x=\omega/\omega_0$ the integral is of the type

$$\mathcal{P}\int_0^\infty \frac{1}{1-x^2}dx = \lim_{\varepsilon\to 0}\left[\int_0^{1-\varepsilon}+\int_{1+\varepsilon}^\infty\right]\left(\frac{1}{1+x}+\frac{1}{1-x}\right)dx = \lim_{\varepsilon\to 0}\left[\ \ln(2-\varepsilon)-\ln(2+\varepsilon)\ \right] = 0.$$

So finally we arrive at the important dispersion relation

$$\Phi(\omega_0) = \frac{2\omega_0}{\pi}\,\mathcal{P}\int_0^\infty \frac{\ln(\rho(\omega))-\ln(\rho(\omega_0))}{\omega_0^2-\omega^2}d\omega\,. \tag{66}$$

6.4 Computation of form factor phase via dispersion relation

6.4.1 Kramers-Kronig phase

The longitudinal form factor is the Fourier transform of the normalized longitudinal charge density distribution

$$\mathcal{F}(\omega) = \int_{-\infty}^\infty \rho(t)e^{i\omega t}dt \quad \text{with} \quad \int_{-\infty}^\infty \rho(t)dt = 1\,. \tag{67}$$

Spectroscopic experiments at particle accelerators yield only the absolute magnitude of the form factor, $F(\omega)=|\mathcal{F}(\omega)|$, but neither its real part nor its imaginary part. Writing

$$\mathcal{F}(\omega) = F(\omega)\exp(i\Phi(\omega)) \tag{68}$$

formula (66) can be applied to compute the phase $\Phi(\omega)$. Physics requires though that we make a slight modification in this formula. Backward transition radiation does not extend to infinite frequencies. High-energy X or gamma rays will never be observed in backward direction. Therefore the upper integration limit in Eq. (69) is far from infinity but rather a suitable cutoff frequency $\omega_{\rm cut}$ in the ultraviolet regime. With this modification the *Kramers-Kronig phase* is given by

$$\boxed{\Phi_{\rm KK}(\omega) = \frac{2\omega}{\pi}\,\mathcal{P}\int_0^{\omega_{\rm cut}} \frac{\ln(|\mathcal{F}(\omega')|)-\ln(|\mathcal{F}(\omega)|)}{\omega^2-\omega'^2}\,d\omega'\,.} \tag{69}$$

provided the prerequisites made in the derivation of this formula are fulfilled. The phase (69) is also called the canonical phase or the minimal phase, the latter expression being somewhat misleading since $\Phi_{\rm KK}(\omega)$ does not correspond to a minimum in the mathematical sense. While there are many test functions obeying the prerequisites there are also important exemptions as will be shown in the next section.

6.4.2 Complex zeros of the form factor, Blaschke product

The most important prerequisite for Eq. (69) to hold is that the form factor must be different from zero in the entire upper half plane ($\Im(\omega_\mathrm{r} + i\omega_\mathrm{i}) = \omega_\mathrm{i} > 0$). If the form factor vanishes at some point inside the closed integration loop Γ its logarithm has a singularity here and the Cauchy Theorem can no longer be applied.

Suppose now that the form factor has a zero at some complex frequency $\omega_1 = a + ib$ in the right upper quarter of the ω plane ($a, b > 0$). An interesting observation is that zeros occur always in pairs, at $\omega_1 = a + ib$ in the right upper quarter and at $\omega_1' = -a + ib$ in the left upper quarter. This can be understood as follows. The charge density is a real function, and using Eq. (67) one finds a relation between the form factor and its complex conjugate: $\mathcal{F}(\omega) = \mathcal{F}^*(-\omega^*)$, which implies that $\omega_1' = -\omega_1^* = -a + ib$ is another zero of $\mathcal{F}(\omega)$. This pair of zeros in the upper half plane can be removed by defining a modified form factor

$$\mathcal{F}_\mathrm{mod}(\omega) = \mathcal{F}(\omega) B(\omega) \tag{70}$$

with the so-called Blaschke factor[5]

$$B(\omega) = \frac{\omega - \omega_1^*}{\omega - \omega_1} \cdot \frac{\omega - \omega_1'^*}{\omega - \omega_1'} = \frac{\omega - (a - ib)}{\omega - (a + ib)} \cdot \frac{\omega - (-a - ib)}{\omega - (-a + ib)} \,. \tag{71}$$

On the real ω axis, the absolute magnitude of the Blaschke factor is 1

$$|B(\omega)| = 1 \quad \Rightarrow \; |\mathcal{F}_\mathrm{mod}(\omega)| = |\mathcal{F}(\omega)| \quad \text{for real} \quad \omega \,. \tag{72}$$

This is a very important equation. It means that the form factor $\mathcal{F}(\omega)$ and the modified form factor $\mathcal{F}_\mathrm{mod}(\omega)$ describe exactly the same radiation spectrum. Knowing just the absolute magnitude from experiment one cannot decide which of the two form factors (or even another expression) is the correct one.

However, the phases of $\mathcal{F}(\omega)$ and $\mathcal{F}_\mathrm{mod}(\omega)$ are different because the Blaschke factor is a complex, frequency-dependent number. Real and imaginary part of $B(\omega)$ are

$$\Re(B(\omega)) = \frac{\omega^4 - 2\omega^2(a^2 + 3b^2) + (a^2 + b^2)^2}{[(\omega - a)^2 + b^2][(\omega + a)^2 + b^2]} \,, \quad \Im(B(\omega)) = \frac{4\omega b(\omega^2 - a^2 - b^2)}{[(\omega - a)^2 + b^2][(\omega + a)^2 + b^2]} \,. \tag{73}$$

The phase of $B(\omega)$ is computed by the equation

$$\Phi_\mathrm{B}(\omega) = \arg(B(\omega)) \,. \tag{74}$$

This phase is not a continuous function of ω but exhibits a discontinuous jump by 2π at the frequency $\omega_\mathrm{jump} = \sqrt{a^2 + b^2}$ where the imaginary part of the Blaschke factor vanishes. It is plotted in Fig. 32 as a function of the real scaled frequency ω/a. The phase jump does not present any problem[6], the equalities $\Re(B(\omega)) = |B(\omega)| \cos \Phi_\mathrm{B}(\omega)$ and $\Im(B(\omega)) = |B(\omega)| \sin \Phi_\mathrm{B}(\omega)$ are perfectly well fulfilled.

In Fig. 33 the function $\Phi_\mathrm{B}(\omega)$ is shown for various ratios b/a. In case of a very small imaginary part of the complex zero $\omega_1 = a + ib$, i.e. for $b/a \ll 1$, the phase excursion $0 \to -\pi \to +\pi \to 0$ is very steep and affects only a narrow frequency range. This means that complex zeros in the immediate vicinity of the real axis have a negligible influence on the bunch shape reconstruction.

[5] The Blaschke correction works for zeros of first order, assuming that in the vicinity of ω_1 the form factor can be expressed as a product of the linar function $(\omega - \omega_1)$ and a function $G(\omega)$ that is nonzero at ω_1.

[6] The situation is rather more complicated if one uses the arctan function instead of the arg function to compute the phase of the Blaschke factor. Then two phase jumps, each by π, are obtained near ω_jump which lead to errors when one computes the sine or cosine of the Blaschke phase. These deficiences can be cured but the mathematical procedure is clumsy.

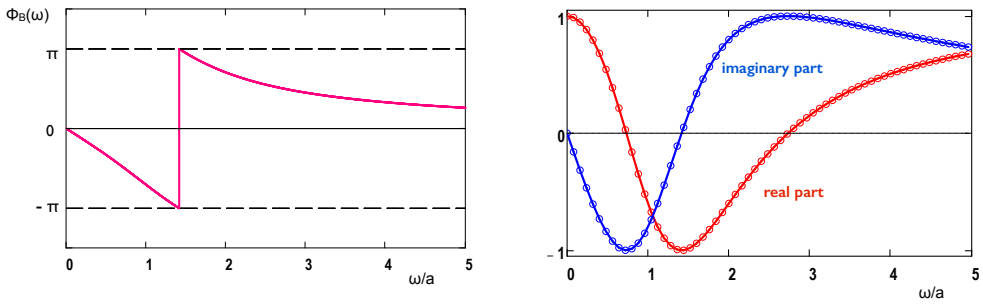

Figure 32: Left: The Blaschke phase $\Phi_{\rm B}(\omega)$ of a pair of zeros (at $\omega_1 = a + ib$ and $\omega_1' = -a + ib$) for a ratio $b/a = 1$. Right: Comparison of $\Re(B(\omega))$ (red curve) with $\cos\Phi_{\rm B}(\omega)$ (red circles) and comparison of $\Im(B(\omega))$ (blue curve) with $\sin\Phi_{\rm B}(\omega)$ (blue circles).

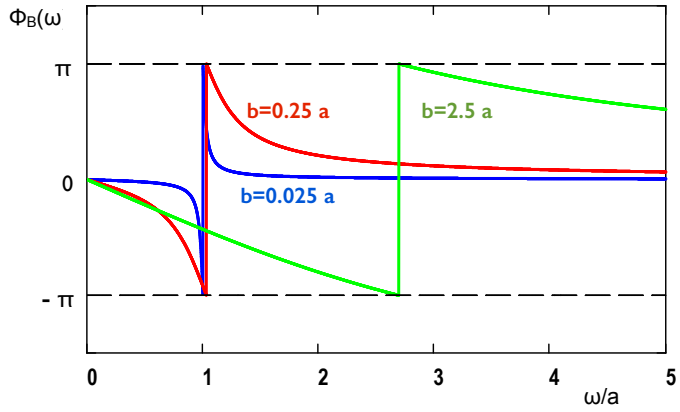

Figure 33: The Blaschke phase $\Phi_{\rm B}(\omega)$ for various ratios b/a.

On the other hand, zeros with a very large imaginary part ($b \gg a$) lead to an almost linearly rising phase at $\omega \approx a$. They do not change the internal structure of the reconstructed bunch but merely shift its position on the time axis.

Suppose now that $\mathcal{F}(\omega)$ has a finite number of pairs of zeros in the upper half of the complex ω plane, at the frequencies $\omega_n = a_n + ib_n$ and $\omega_n' = -a_n + ib_n$. The *Blaschke product* is defined as the product of the Blaschke factors $B_n(\omega)$ of these pairs. The phases are additive.

$$B(\omega) = \prod_n B_n(\omega) = \prod_n \frac{\omega - (a_n - ib_n)}{\omega - (a_n + ib_n)} \cdot \frac{\omega - (-a_n - ib_n)}{\omega - (-a_n + ib_n)}\,, \qquad \Phi_{\rm B}(\omega) = \sum_n \Phi_{{\rm B},n}(\omega)\,. \tag{75}$$

In analogy with Eq. (70) the modified form factor is given by

$$\mathcal{F}_{\rm mod}(\omega) = \mathcal{F}(\omega) B(\omega)\,. \tag{76}$$

This form factor has no zero in the upper half plane. It fulfills the requirements made in the derivation of formula (69), and hence the phase of the modified form factor is identical with the Kramers-Kronig phase $\Phi_{\rm KK}(\omega)$. The phase of our original form factor follows immediately from Eq. (76)

$$\Phi(\omega) = \Phi_{\rm KK}(\omega) - \Phi_{\rm B}(\omega)\,. \tag{77}$$

6.5 Probing the Kramers-Kronig and Blaschke phase

We have shown in Eq. (72) that multiplying a form factor $\mathcal{F}(\omega)$ with a Blaschke factor $B(\omega)$ leads to a new form factor $\mathcal{F}_{\rm mod}(\omega)$ which has the same absolute magnitude $F(\omega)$ on the real axis. Since the Kramers-Kronig phase is computed from $F(\omega)$ there are necessarily ambiguities in the reconstruction of the time signal. Akutowicz [25] proved that a unique reconstruction of a function from the magnitude of its Fourier transform is indeed impossible. A simple counter example demonstrates this in a convincing way. Two functions $f_1(t)$ and $f_2(t)$ are considered which vanish for $t < 0$ and which for $t \geq 0$ are given by

$$\begin{aligned} f_1(t) &= e^{-\beta t} \\ f_2(t) &= e^{-\beta t}\left(1 + \frac{4\beta^2(1-\cos(\alpha t))}{\alpha^2} - \frac{4\beta\sin(\alpha t)}{\alpha}\right) \end{aligned}$$

with real parameters $\alpha, \beta > 0$. The first function has an infinitely steep rise at $t = 0$, followed by an

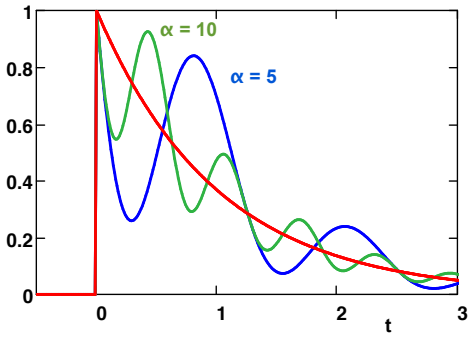

Figure 34: The Akutowicz functions $f_1(t)$ (red) and $f_2(t)$ for $\beta = 1$ and $\alpha = 5$ (blue) resp. $\alpha = 10$ (green).

exponential decay. The second function has the same steep rise but the decay is superimposed with an oscillatory pattern, see Fig. 34. The complex form factors $\mathcal{F}_1(\omega)$ and $\mathcal{F}_2(\omega)$ differ considerably

$$\mathcal{F}_1(\omega) = \frac{1}{\beta + i\omega}\,, \qquad \mathcal{F}_2(\omega) = \frac{\alpha^2 + (\beta + i\omega)^2}{[\alpha^2 + (\beta - i\omega)^2](\beta - i\omega)} \tag{78}$$

but surprisingly their absolute magnitudes are identical on the real ω axis

$$|\mathcal{F}_1(\omega)| = |\mathcal{F}_2(\omega)| = \frac{1}{\sqrt{\beta^2 + \omega^2}} \quad \text{for real } \omega\,. \tag{79}$$

The phases are

$$\Phi_1(\omega) = \arg(\mathcal{F}_1(\omega))\,, \quad \Phi_2(\omega) = \arg(\mathcal{F}_2(\omega))\,. \tag{80}$$

Signal reconstruction using the Kramers-Kronig and Blaschke phase
The KK method reproduces the function $f_1(t)$ very accurately, see Fig. 35, and also the phase is reproduced quite well. However, any attempt to reconstruct the oscillatory function $f_2(t)$ must fail, no matter what the value of α is.

Now we investigate whether the Blaschke phase in combination with the KK phase enables a faithful reconstruction of $f_2(t)$. To this end we have to find the complex zeros of the form factor $\mathcal{F}_2(\omega)$. This

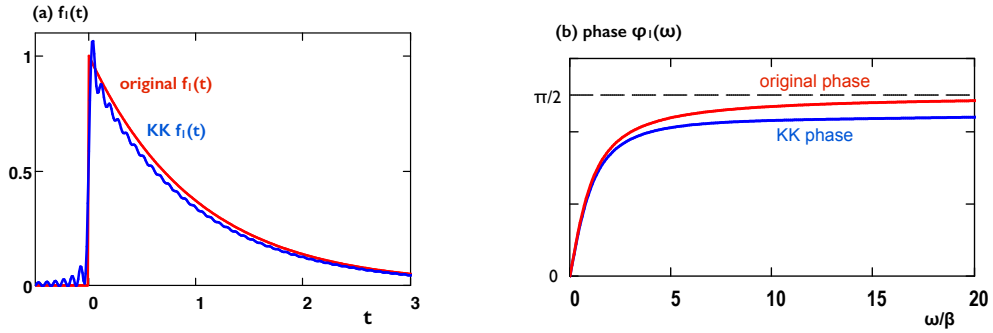

Figure 35: **(a)** The function $f_1(t)$ (red) and its Kramers-Kronig reconstruction (blue). **(b)** The phase $\Phi_1(\omega)$ of the complex form factor $\mathcal{F}_1(\omega)$ (red) and the Kramers-Kronig phase $\Phi_{\rm KK}(\omega)$ (blue).

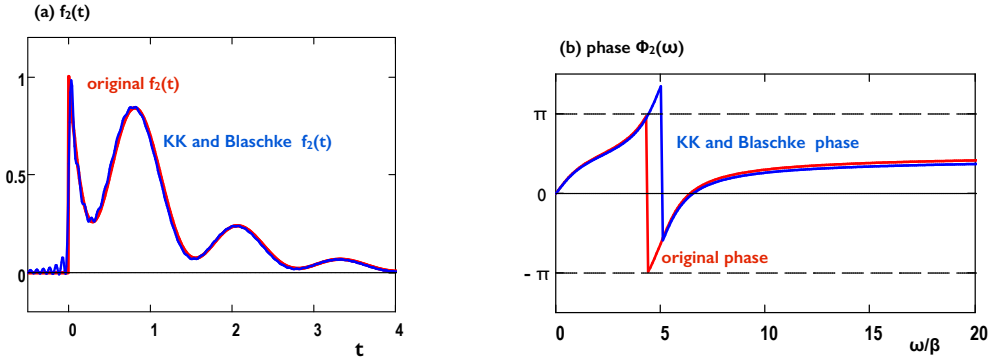

Figure 36: **(a)** The function $f_2(t)$ (red) and its reconstruction (blue) using the Kramers-Kronig phase $\Phi_{\rm KK}(\omega)$ and the Blaschke phase $\Phi_{\rm B}(\omega)$. **(b)** The reconstruction phase $\Phi_{\rm rec}(\omega) = \Phi_{\rm KK}(\omega) - \Phi_{\rm B}(\omega)$ (blue curve) in comparison with the phase $\Phi_2(\omega)$ of the form factor $\mathcal{F}_2(\omega)$ (red curve).

is easy: the numerator of $\mathcal{F}_2(\omega)$ must vanish if we insert the complex frequency $\omega_1 = a + ib$:

$$0 = \alpha^2 + (\beta + i\omega_1)^2 = \alpha^2 + (\beta + ia - b)^2 = \alpha^2 + \beta^2 - a^2 + b^2 - 2b\beta + i\,2a(\beta - b)\,.$$

Both real and imaginary part of this equation must be zero. From this condition follows immediately

$$b = \beta\,, \qquad a = \pm\alpha\,.$$

The form factor $\mathcal{F}_2(\omega)$ has just one pair of zeros in the upper half plane: $\omega_1 = \alpha + i\beta$ in the right upper quarter of the complex ω plane and its mirror image $\omega_1' = -\alpha + i\beta$ in the left upper quarter. We consider the function $f_2(t)$ with $a = \alpha = 5$ and $b = \beta = 1$. Using the results of Sect. 6.4.2 we compute the Blaschke phase $\Phi_{\rm B}(\omega)$ with the parameters $a = 5$ and $b = 2$. The reconstruction phase $\Phi_{\rm rec}(\omega) = \Phi_{\rm KK}(\omega) - \Phi_{\rm B}(\omega)$ agrees very well with the original phase $\Phi_2(\omega)$ of the form factor $\mathcal{F}_2(\omega)$, see Fig. 36b. When we use this phase to compute the function $f_2(t)$ from the magnitude $|\mathcal{F}_2(\omega)|$ of the Fourier we find perfect agreement with the original function (Fig. 36a). In our view this is a remarkable success of the dispersion relation theory.

7 Appendix B: Model Calculations

Bernhard Schmidt, Peter Schmüser et al., preliminary version

To assess the capabilities and the limitations of the phase reconstruction of the bunch form factor by dispersion relation it is useful to employ the method for simple test functions $\rho(t)$ whose complex form factor is either known analytically or can be calculated by Fourier transfomation. In this section the variables t and ω have a dimension. Time t is measured in picoseconds (10^{-12} s), frequency $f = \omega/(2\pi)$ in Terahertz (10^{12} Hz). For brevity, the circular frequency $\omega = 2\pi f$ is called "frequency" in the following.

7.1 Single Gaussian and truncated cosine

Let the normalized charge density and its Fourier transform be given by

$$\rho(t) = \frac{1}{\sqrt{2\pi}\,\sigma_t}\,\exp\left(-\frac{t^2}{2\sigma_t^2}\right)\,, \quad \mathcal{F}(\omega) = \exp\left(-\frac{\omega^2}{2\sigma_\omega^2}\right) \quad \text{with} \quad \sigma_\omega = \frac{1}{\sigma_t}\,. \tag{81}$$

With the Gaussian Fourier transform we are facing a mathematical problem. The logarithm is proportional to the square of frequency, $\ln(|\mathcal{F}(\omega)|) \propto \omega^2$, which means that the integral over the large semicircle Γ_1 diverges, compare expression (61). This deficiency, however, is easy to cure: one truncates the Gaussian at a sufficiently large frequency $\omega_{\rm tr}$ and extrapolates it with an inverse power law. For example

$$\begin{aligned} \mathcal{F}(\omega) &= \exp\left(-\frac{\omega^2}{2\sigma_\omega^2}\right) \quad \text{for} \quad 0 \le \omega < \omega_{\rm tr}\,, \\ \mathcal{F}(\omega) &= \exp\left(-\frac{\omega_{\rm tr}^2}{2\sigma_\omega^2}\right)\,\frac{\omega_{\rm tr}^{10}}{\omega^{10}} \quad \text{for} \quad \omega_{\rm tr} \le \omega < \infty\,. \end{aligned} \tag{82}$$

The extrapolation is shown in Fig. 37. With this extrapolation all requirements of the derivation of Eq. (69) are fulfilled. The effect on the bunch shape is hardly noticeable.

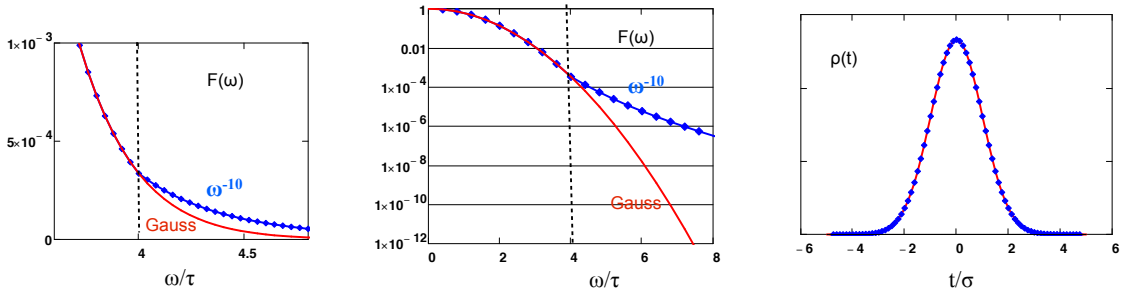

Figure 37: Replacing the tail of a Gaussian form factor by an inverse power law: $\mathcal{F}(\omega) \propto 1/\omega^{10}$. The original charge distribution $\rho(t)$ (red curve) and the charge distribution derived from the modified form factor (blue dots) are almost identical.

Having this small correction in mind we are justified using Gaussians in our model calculations. The Kramers-Kronig phase computed with Eq. (69) from $|\mathcal{F}(\omega)|$ agrees perfectly with the known analytical phase of $\mathcal{F}(\omega)$ (both are identical to zero for a Gaussian bunch centered at $t = 0$). Also the original and the reconstructed charge distribution are in perfect agreement.

Another useful model function for a bunch exhibiting only one maximum is a cosine wave restricted to the interval $-b \le t \le b$.

$$\rho(t) = \frac{1}{2b}\left[1 + \cos\left(\frac{\pi}{b}\,t\right)\right] \quad \text{for} \quad 0 \le t \le b\,, \quad \rho(t) = 0 \quad \text{otherwise}\,. \tag{83}$$

Also in this case the Fourier transform is known analytically:

$$\mathcal{F}(\omega) = \frac{\pi^2 \sin(\omega b)}{\omega b(\omega^2 b^2 - \pi^2)}\,. \tag{84}$$

This form factor has the nice feature that it drops like $1/\omega^3$ at large frequency and thus fulfills the condition (61). The Kramers-Kronig phase reconstruction works well, and the reconstructed charge distribution agrees almost perfectly with the input distribution (Fig. 38).

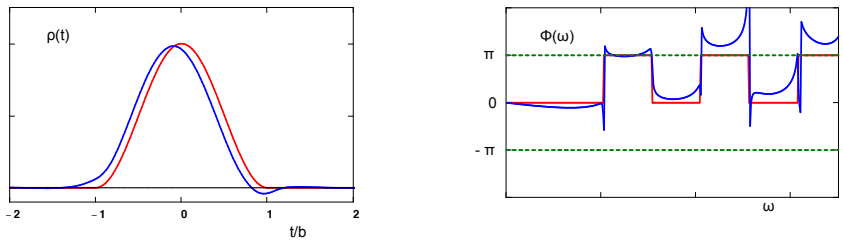

Figure 38: Left: A cosine-shaped bunch (red) and its KK reconstruction (blue). Right: Analytical and KK phase.

When the Gaussian or cosine-like bunches are not centered at $t = 0$ but at some time $t = t_c \neq 0$ the form factors aquire an additional phase factor:

$$\rho(t) = \frac{1}{\sqrt{2\pi}\,\sigma_t}\,\exp\left(-\frac{(t-t_c)^2}{2\sigma_t^2}\right) \quad \Rightarrow \quad \mathcal{F}(\omega) = \exp\left(-\frac{\omega^2}{2\sigma_\omega^2}\right)\exp(+i\omega t_c)\,. \tag{85}$$

7.2 Bunch profiles with two or three peaks

When the Kramers-Kronig phase reconstruction is applied for bunches with several peaks one obtains puzzling results: in some cases the original is perfectly reproduced, in other cases the reconstructed charge distribution is very different from the original. This will be illustrated with a number of examples, and we show the benefit of the Blaschke phase correction.

Two Gaussians

Let the bunch shape be given by the sum of two well-separated Gaussians of different width. This example has been discussed previously, see Fig. 13 in sect. 3.3.4. The reconstruction is good if the narrow peak comes first, but the sequence of the reconstructed peaks is interchanged when the wide peak comes first. This interchange is easy to understand. The charge density $\rho(t)$ is a real function, so from Eq. (67) follows immediately that the absolute magnitude of the form factor $F(\omega) = |\mathcal{F}(\omega)|$ is also an even function of ω while the phase is an odd function:

$$F(-\omega) = +F(+\omega)\,, \quad \Phi(-\omega) = -\Phi(+\omega)\,. \tag{86}$$

An interchange of the two Gaussians corresponds to a time inversion and is equivalent to a sign reversal of ω. This leaves the absolute magnitude of the form factor invariant and has thus no effect on the phase (69).

Problems arise, when the two peaks are rather close to each other, as has been shown in Fig. 13. Similar difficulties are observed for three Gaussians of different width and will be discussed in the next section.

Three Gaussians

Serious problems arise for a bunch profile consisting of three Gaussians with increasing width. Here an interchange of the first two peaks leads to a reconstructed shape in which not only the time order of the first two peaks is inverted but in addition their shape is modified. Similar difficulties were reported in [34].

We study now a charge distribution consisting of three Gaussians

$$\rho(t) = \frac{1}{A_1 + A_2 + A_3} \sum_{n=1}^{3} \frac{A_n}{\sqrt{2\pi}\,\sigma_{t,n}} \exp\left(-\frac{(t-t_c)^2}{2\sigma_{t,n}^2}\right) \tag{87}$$

The form factor and its analytical phase are

$$\mathcal{F}(\omega) = \frac{1}{A_1 + A_2 + A_3} \sum_{n=1}^{3} \exp\left(-\frac{\omega^2}{2\sigma_{\omega,n}^2}\right) e^{i\omega t_n}\,, \quad \Phi(\omega) = \arg(\mathcal{F}(\omega))\,. \tag{88}$$

Three different parameter sets are considered.

Example 1: Three Gaussians of equal width and uniform spacing

We choose $\sigma_{t,1} = \sigma_{t,2} = \sigma_{t,3} = 0.1\,\text{ps}$ and $t_2 - t_1 = t_3 - t_2 = 0.45\,\text{ps}$ but admit different amplitudes. Figure 39 shows that the KK reconstruction of the charge distribution and of the phase is almost perfect if the highest peak is at the front (amplitudes $A_1 = 1.0$, $A_2 = 0.5$, $A_3 = 0.3$).

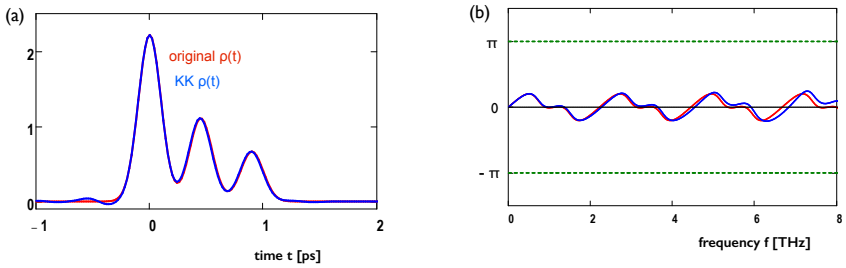

Figure 39: Three Gaussians of equal width and with uniform spacing, the largest peak is at the front. (a): Original and reconstructed charge distribution $\rho(t)$. (b). The analytical phase $\Phi(\omega)$ of the form factor $\mathcal{F}(\omega)$ (red) and the Kramers-Kronig phase Φ_{KK} (blue).

Quite a different result is obtained if the highest peak is in the center (amplitudes $A_1 = 0.5$, $A_2 = 1.0$, $A_3 = 0.3$). The KK reconstruction disagrees with the input distribution as shown in Fig. 40. The highest peak appears at the front instead of in the center. This is quite a typical result, the Kramers-Kronig method has a tendency to move the most pronounced spike to the front.

The question is: what is the reason for such "false" reconstructions? We will demonstrate that zeros of the form factor in the upper half of the complex ω plane are responsible for these discrepancies. These zeros are determined by plotting the contour lines $\Re(\mathcal{F}(\omega)) = 0$ and $\Im(\mathcal{F}(\omega)) = 0$ in the complex ω plane and finding their intersection points in the upper half plane. The numerical results are shown

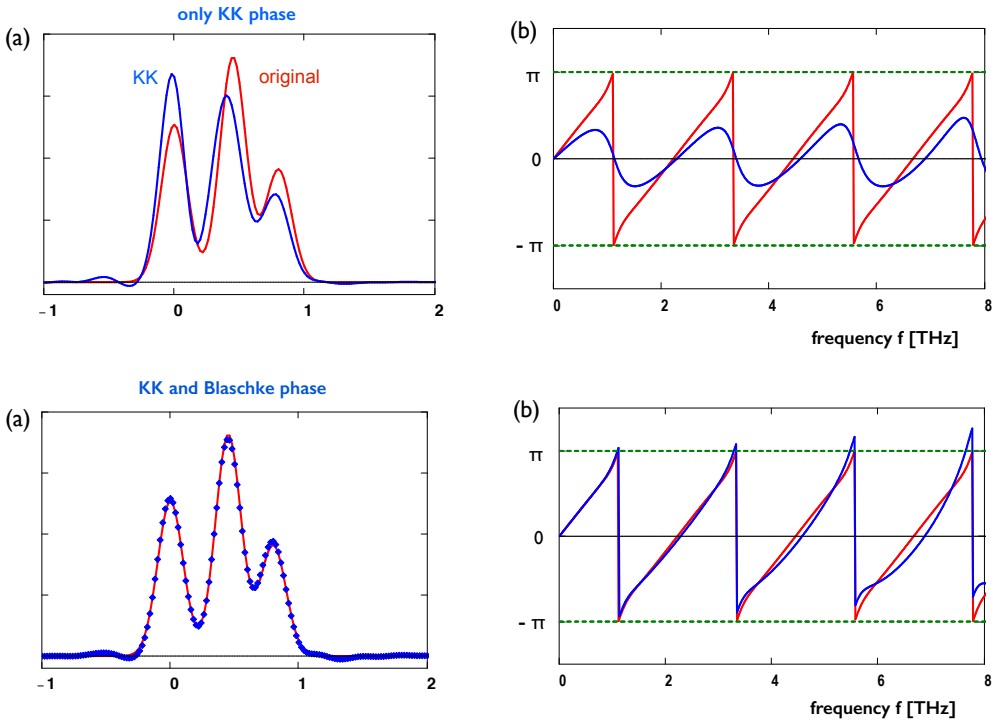

Figure 40: Three Gaussians of equal width and with uniform spacing, the largest peak is in the center. *Top :* Only KK phase used: poor reconstruction. *Bottom :* KK phase and Blaschke phase taken into consideration: perfect reconstruction of charge distribution and phase.

in Fig. 41. The crossing points give us the complex zeros $\omega_n = a_n + ib_n$ which are needed to compute the Blaschke phase $\Phi_{\rm B}(\omega)$.

In this Example 1 we take 9 complex zeros $\omega_n = a_n + ib_n$ into account which are located in the right upper quarter of the ω plane, and in addition their mirror images $\omega_n' = -a_n + ib_n$ in the left upper quarter. The total Blaschke phase and the reconstruction phase become

$$\Phi_{\rm B}(\omega) = \sum_{n=1}^{9} \Phi_{B,n}(\omega)\,, \quad \Phi_{\rm rec}(\omega) = \Phi_{\rm KK}(\omega) - \Phi_{\rm B}(\omega)\,.$$

Figure 40 shows that this phase agrees very well with the analytical phase of the form factor $\mathcal{F}(\omega)$, and that the reconstructed charge distribution is almost identical with the original one.

Why don't we need a Blaschke phase in case 1 ?
We have just shown that in the first case (largest peak at the front) an excellent reconstruction of the initial distribution is achieved using the KK phase alone, while in the second case (largest peak in the center) the KK phase is insufficient and the Blaschke phase is needed as well. Why don't we have to use the Blaschke phase in the first case? Would it improve or rather spoil the reconstruction? The answer is found by looking at the contour plots in Fig. 41. If the maximum is at the front the form factor does not have any zeros in the upper half of the complex ω plane, hence the Blaschke phase is indeed zero. However, if the maximum is in the center one finds a sequence of form factor zeros in the upper half plane which give rise to a nonvanishing Blaschke phase.

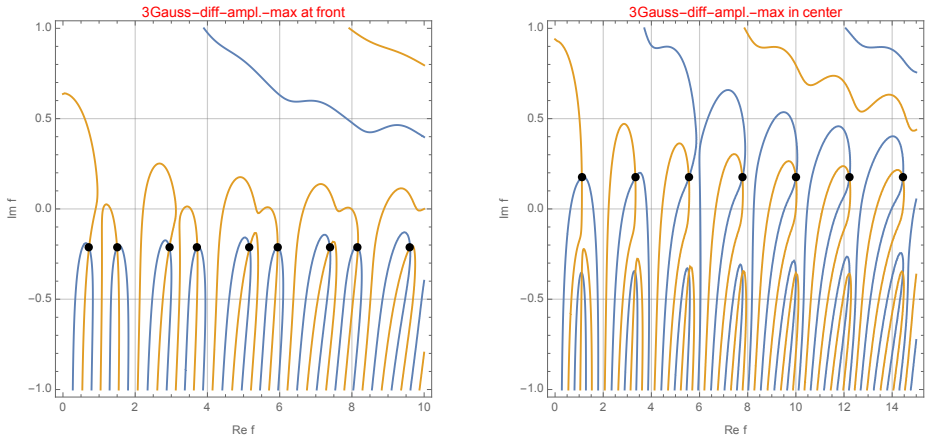

Figure 41: Three Gaussians of different amplitude. Plotted are the contour lines $\Re(\mathcal{F}(\omega)) = 0$ (blue) and $\Im(\mathcal{F}(\omega)) = 0$ (yellow) in the complex ω plane. The dots indicate the crossing points where the absolute magnitude of the form factors vanishes. *Left plot*: Large peak at the front. There are no zeros in the upper half of the complex ω plane, hence the Blaschke phase is zero. *Right plot*: Large peak in the center. There is a sequence of zeros in the upper half plane which contribute to the Blaschke phase.

Example 2: Three Gaussians of equal width but variable spacing

We choose again $\sigma_{t,n} = 0.1\,\text{ps}$ and amplitudes $A_1 = 0.7, A_2 = 1.0, A_3 = 0.5$ such that the highest peak is in the center. In comparison with the previous example the first and third peak are somewhat

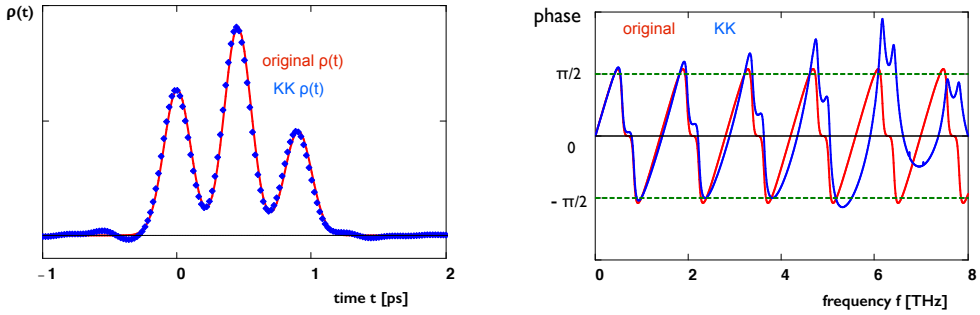

Figure 42: Left: A bunch consisting of three Gaussians of equal width and with uniform spacing ($t_2 - t_1 = t_3 - t_2 = 0.45\,\text{ps}$). Red curve: original $\rho(t)$, blue curve: KK reconstruction. Right: The original phase $\Phi(\omega)$ (red) and the Kramers-Kronig phase $\Phi_{\text{KK}}(\omega)$ (blue).

higher which has the interesting consequence that the KK reconstruction is good provided the peaks are equidistant, see Fig. 42. For uniform spacing, both the input charge distribution and the phase are remarkably well reproduced by the KK method.

However, a totally different result is obtained for non-uniform spacing. The reconstructed bunch profile differs considerably from the original profile, again the largest peak appearing at the front and not in the center of the bunch see Fig. 43. The KK-phase reproduces the analytical phase rather poorly. How can one improve the reconstrucion? Again we determine numerically the form factor zeros in the upper half plane and compute the Blaschke phase. The result is also shown in Fig. 43.

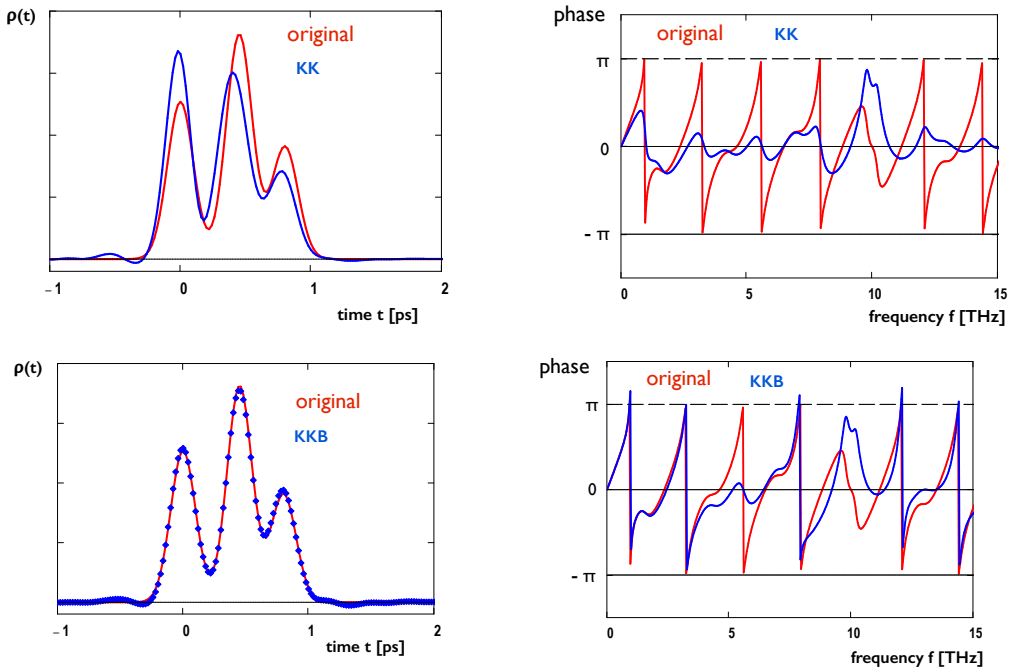

Figure 43: *Top left:* A bunch consisting of three Gaussians of equal width and non-uniform spacing ($t_2 - t_1 = 0.45\,\text{ps}$, $t_3 - t_2 = 0.35\,\text{ps}$). Red curve: original $\rho(t)$, blue curve: KK reconstruction. *Top right:* The original phase $\Phi(\omega)$ and the computed KK phase $\Phi_{\text{KK}}(\omega)$. *Bottom left:* The same bunch consisting of three Gaussians (red) and its reconstruction using the Kramers-Kronig and Blaschke phases (blue). *Bottom right:* The original phase $\Phi(\omega)$ and the reconstruction phase $\Phi_{\text{rec}}(\omega) = \Phi_{\text{KK}}(\omega) - \Phi_{\text{B}}(\omega)$.

The reconstruction phase $\Phi_{\text{rec}}(\omega) = \Phi_{\text{KK}}(\omega) - \Phi_{\text{B}}(\omega)$ agrees very well with the phase $\Phi(\omega)$ of the form factor $\mathcal{F}(\omega)$ and the charge distribution is perfectly reconstructed. Again it is instructive to compare the contour plots for the two cases: uniform spacing (left plot in Fig. 44) and non-uniform spacing (right plot in Fig. 44). When the KK phase alone is sufficient for reconstruction (case 1) all complex zeros are in the lower half plane, hence the Blaschke phase vanishes. In case 2, where the KK phase alone yields an unsatisfactory reconstruction, the complex zeros are in the upper half plane and contribute to the Blaschke phase.

Example 3: Three Gaussians of different widths

In the previous examples the incorporation of the Blaschke phase leads to an almost perfect reconstruction of the longitudinal charge distribution. Now we study a less favorable case, namely three Gaussians with different standard deviations. When the narrowest peak at the front the KK method works very well, see Fig. 45.

Not surprisingly in view of our previous results is the observation that the situation changes drastically when the most pronounced structure, in this case the narrow peak, is in the center. The KK

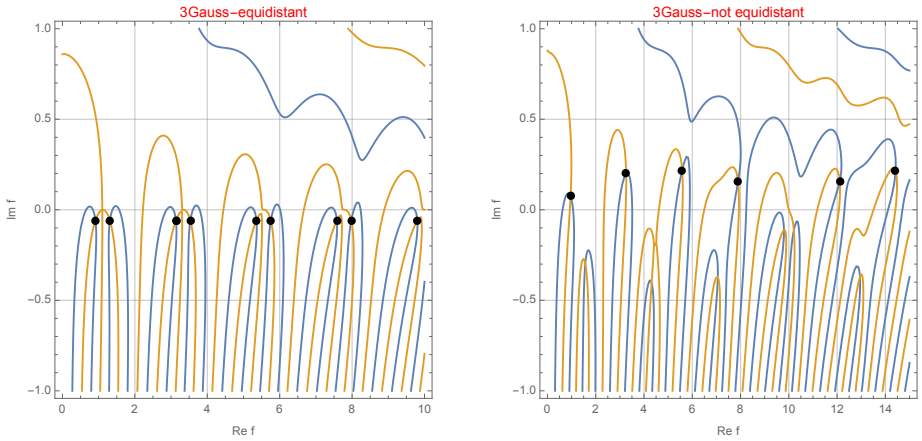

Figure 44: Three Gaussians of variable spacing. Shown are the contour lines $\Re(\mathcal{F}(\omega)) = 0$ (blue) and $\Im(\mathcal{F}(\omega)) = 0$ (yellow) in the complex ω plane. The dots indicate the crossing points where the absolute magnitude of the form factors vanishes. *Left plot*: Peaks are uniformly spaced. There are no zeros in the upper half of the complex ω plane, hence the Blaschke phase is zero. *Right plot*: Peaks are not uniformly spaced. There is a sequence of zeros in the upper half plane which contribute to the Blaschke phase.

reconstruction yields a distribution with the narrow peak at the front. The Blaschke correction turns out to be tedious. As shown in Fig. 47 there are an enormous number of densely spaced complex zeros, which moreover are not close to the real axis but oriented along a diagonal. The total Blaschke phase, Eq. (75), contains very many terms. In Fig. 46 we have taken 48 zeros into account and get an acceptable though not fully satisfactory reconstruction.

The convergence is slow. To demonstrate this we show in Fig. 48 the reconstruction with 6 or 24 terms in Eq. (75).

7.3 Conclusions

The Examples 1, 2 and 3 demonstrate the great potential of Complex Analysis for determing the phase of the form factor. The ambiguities in signal reconstruction that are frequently observed in model calculations based on the Kramers-Kronig phase alone can be eliminated when in addition the Blaschke phase is taken into consideration. Unfortunately our investigations on the Blaschke phase are more of an academic nature and cannot be utilized for retrieving the phase of the form factor of a real electron bunch in the linac from spectroscopic measurements: there is simply no experimental information available about zeros of the form factor in the complex ω plane.

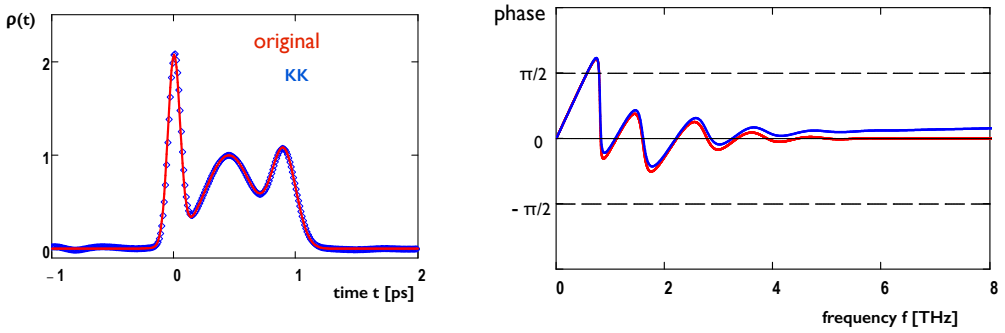

Figure 45: Left: A bunch consisting of three Gaussians of different width ($\sigma_1 = 0.05\,\text{ps}$, $\sigma_2 = 0.2\,\text{ps}$, $\sigma_1 = 0.1\,\text{ps}$). The original charge distribution $\rho(t)$ (red curve) and the KK reconstruction (blue curve) are in excellent agreement. Right: The original phase $\Phi(\omega)$ (red) and the Kramers-Kronig phase $\Phi_{\text{KK}}(\omega)$ (blue) agree too.

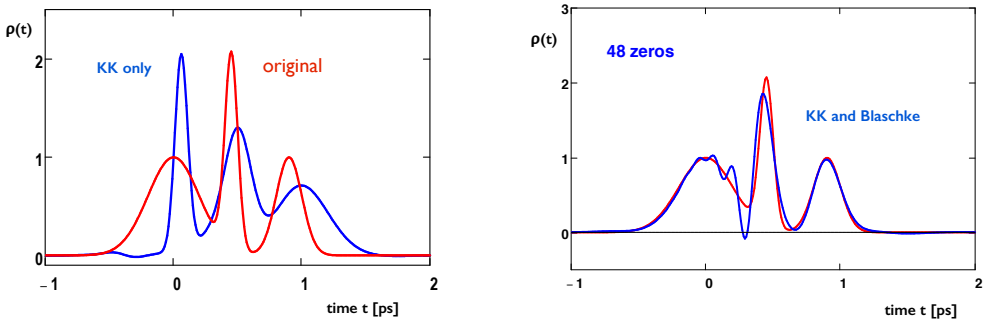

Figure 46: Left: A bunch consisting of three Gaussians of different width ($\sigma_1 = 0.2\,\text{ps}$, $\sigma_2 = 0.05\,\text{ps}$, $\sigma_1 = 0.1\,\text{ps}$) with the narrow peak in the center. The original charge distribution $\rho(t)$ (red curve) and the KK reconstruction (blue curve) are very different. Right: Reconstructed charge distribution (blue) using the Kramers-Kronig phase and the Blaschke phase (computed for 48 zeros).

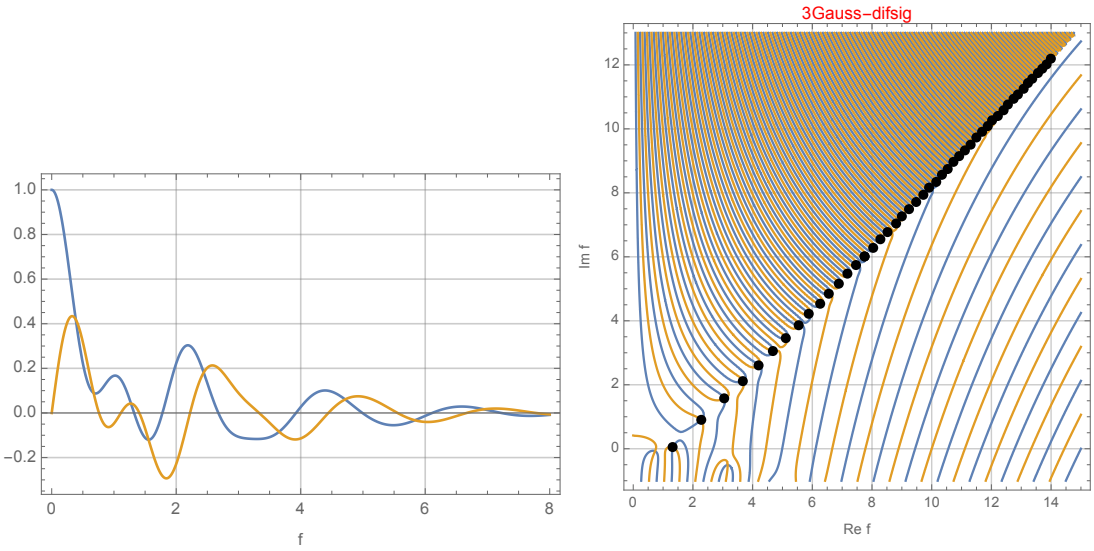

Figure 47: Three Gaussians of different width. *Left*: The real and imaginary part of the form factor plotted as functions of the real frequency $f = \omega/2\pi$. *Right*: The contour lines $\Re(\mathcal{F}(\omega)) = 0$ (blue) and $\Im(\mathcal{F}(\omega)) = 0$ (yellow) in the complex ω plane. There are an enormous number of densely spaced complex zeros.

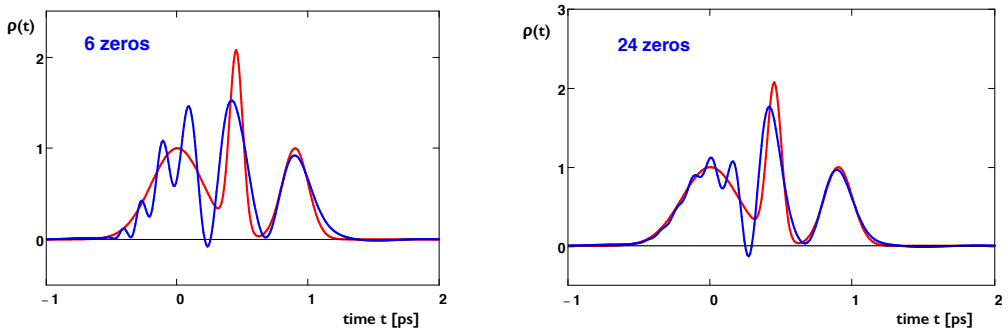

Figure 48: Reconstruction using the Kramers-Kronig and Blaschke phases with 6 resp. 24 complex zeros.